

Preparation and Characterization of Lamellar Vanadyl Alkylphosphates as Catalyst Precursors for the Selective Oxidation of Butane

Yuichi Kamiya,* Eiichiro Nishikawa, Atsushi Satsuma,† and Toshio Okuhara††

Research and Development Center, Tonen Chemical Corporation, 3-1 Chidori-cho, Kawasaki-ku, Kawasaki 210-0865

†Department of Applied Chemistry, Graduate School of Engineering, Nagoya University, Nagoya 464-8603

††Graduate School of Environmental Earth Science, Hokkaido University, Sapporo 060-0810

(Received August 7, 2002)

Vanadyl alkylphosphates consisting of V^{4+} and P^{5+} were synthesized by the reaction of a solid mixture of V_2O_5 and V_4O_9 (2:3 in mol) with P_2O_5 in primary aliphatic (from C_1 to C_8), secondary aliphatic (C_3 and C_4), and alicyclic (C_5) alcohols, and were characterized by means of elemental analysis, thermogravimetric analysis, X-ray diffraction, IR spectroscopy, and magnetic susceptibility. The chemical formulae of the products were determined to be $VO(RO)_x(HO)_{1-x}PO_3 \cdot (ROH)_y$ ($x = 0.5$–0.7, $y = 0.3$–0.5 for primary aliphatic alcohols; $x = 0.1$–0.2, $y = 0.4$–0.9 for secondary aliphatic and alicyclic alcohols; and R = organic group). X-ray diffraction revealed that the compounds had a lamellar structure, where the organic groups existed as double layers with a tilt of about 56° against the basal plane. Magnetism and IR spectroscopy demonstrated that the construction of the basal planes in the vanadyl alkylphosphates was similar to that of $VOHPO_4 \cdot 0.5H_2O$, which consists of V^{4+} dimers linked with PO_4, except for vanadyl *sec*-butylphosphate, consisting of isolated V^{4+} monomers. Calcination of vanadyl methylphosphate and vanadyl cyclopentylphosphate brought about crystallites of $(VO)_2P_2O_7$. These $(VO)_2P_2O_7$ exhibited high selectivities to maleic anhydride (65–68%) for the selective oxidation of butane under a high concentration of butane (5.0%).

The selective oxidation of butane to maleic anhydride (abbreviated as MA) is an important commercial process, because MA is a useful raw material for agricultural chemicals, food additives, and unsaturated polymer resins. Furthermore, this reaction presently has only a few commercialized applications in the gas-solid catalytic oxidations of lower alkanes with molecular oxygen.[1] Vanadyl pyrophosphate, $(VO)_2P_2O_7$, is claimed to be an efficient phase for this reaction, and is a main component of the commercial catalyst.[2–4] The $(VO)_2P_2O_7$ catalyst is usually formed by a topotactic transformation of $VOHPO_4 \cdot 0.5H_2O$,[5,6] which is a prevailing precursor. So far, there have been many reports on the preparation methods, preparation conditions, and activation processes.[7–9] However, since the yields are limited to about 55%, further improvement of the yield is still desired. A new precursor is indispensable for the development of an effective catalyst.

A series of vanadium phosphorus (V–P) oxides have attracted a great deal of attention, because of their structural diversity and unique catalytic property. So far, there are many reports on the various V–P oxides, such as lamellar compounds,[10–16] large crystallites,[17] mesostructured materials,[18–21] and thin-layer compounds.[22–24] Lamellar compounds are demonstrated by vanadyl alkylphosphonates and alkylphosphates consisting of alternating inorganic V–P–O layers and organic group ones. Vanadyl alkylphosphonates are shown by $VO(RPO_3) \cdot nH_2O$, in which the oxidation numbers of V and P are +4 and +3, respectively, and R is an alkyl group. These compounds contain P–C bonds. Johnson et al. synthesized a number of vanadyl alkylphosphonates from V_2O_5 and a variety of corresponding alkylphosphonic acid, $RPO(OH)_2$.[12–14,16] Guliants et al. claimed that vanadyl methylphosphonate was transformed to $(VO)_2P_2O_7$ by calcination.[11]

On the contrary, there are only few reports about vanadyl alkylphosphates, in which ester bonds of (O=)P–O–C are included, and V and P are 4+ and 5+, respectively. Researchers of DuPont described vanadyl alkylphosphates synthesized by the reaction of V_2O_5 with P_2O_5 in alcohol.[10] However, the incorporated alkylphosphates are limited to only those obtained from primary aliphatic alcohols. In addition, the structure has been insufficiently characterized.

We reported in a previous communication that vanadyl alkylphosphates incorporating various alkylphosphates can be synthesized by the reaction of partially reduced V_2O_5 with P_2O_5 in alcohols including secondary aliphatic and alicyclic alcohols.[25] The catalyst obtained by the calcination of vanadyl methylphosphate showed a high catalytic performance for the selective oxidation of butane,[25] demonstrating that these vanadyl alkylphosphates are promising starting materials for the catalysts.

In the present study, the vanadyl alkylphosphates were synthesized, and were systematically characterized by means of elemental analysis, X-ray diffraction, IR spectroscopy, thermogravimetric analysis, and magnetic susceptibility. The catalytic properties of the V–P oxides obtained from these vanadyl alkylphosphates were investigated for the selective oxidation of butane. Their catalytic performance is discussed in relation to microstructure of the catalyst crystallites.

Experimental

Materials. Vanadyl alkylphosphates were prepared as follows.[25] V_2O_5 (29.2 g (0.16 mol), Koso Chemical Co., Ltd.) was reduced with

a mixture of isobutyl alcohol (180 cm^3, Koso Chemical Co., Ltd.), and benzyl alcohol (120 cm^3, Koso Chemical Co., Ltd.) at the refluxing temperature (387 K) for 3 h. The obtained black solid was separated by filtration. The powder XRD pattern revealed that this solid was a mixture of V_2O_5 and V_4O_9. The average oxidation number of V was determined by a titration method[26] to be +4.73, indicating that V_2O_5 and V_4O_9 coexisted at a molar ratio of 2:3. The obtained $V_2O_{4.73}$ (20 g) was added to 300 cm^3 of each alcohol. The following primary aliphatic alcohols were used: methanol, ethanol, 1-propanol, 1-butanol (Koso Chemical Co., Ltd.), 1-hexanol, and 1-octanol (Tokyo Kasei Kogyo Co., Ltd.). The secondary alcohols were: aliphatic alcohol; 2-propanol and 2-butanol (Koso Chemical Co., Ltd.), and alicyclic alcohol; cyclopentanol (Tokyo Kasei Kogyo Co., Ltd.). A mixture of P_2O_5 (29.6 g (0.21 mol), Koso Chemical Co., Ltd.) and toluene (70 cm^3, Koso Chemical Co., Ltd.) was slowly added to an alcoholic suspension with stirring at room temperature. The mixture was then refluxed until the color of the suspension changed to light blue, e.g., methanol (80 h), ethanol (30 h), 1-propanol (18 h), 1-butanol (3 h), 1-hexanol (2 h), 1-octanol (2 h), 2-propanol (40 h), and cyclopentanol (20 h). In the case of 2-butanol, the mixture was refluxed for 100 h, and a greenish-brown suspension was obtained instead of a light-blue suspension. The resulting vanadyl alkylphosphates were separated by filtration, washed with acetone and dried at room temperature for 16 h. Hereafter, these vanadyl alkylphosphates will be denoted as VAP–*alcohol name*, e.g., VAP–*methanol*.

As a reference, vanadyl hydrogen phosphate hemihydrate, $VOHPO_4 \cdot 0.5H_2O$, was prepared according to the literature.[27] V_2O_5 (14.7 g (0.08 mol)) was added to a mixture of 90 cm^3 of isobutyl alcohol and 60 cm^3 of benzyl alcohol. The suspension was refluxed at 387 K for 3 h, and cooled to room temperature. 99% H_3PO_4 (15.8 g (0.16 mol), MERCK Ltd.) was added to the suspension, followed by refluxing at 387 K for 3 h. The resulting solid was filtered, washed with acetone and dried at room temperature for 16 h. The XRD pattern of this material was in good agreement with that of $VOHPO_4 \cdot 0.5H_2O$ reported in the literature.[27,28]

Characterization. XRD patterns were recorded on an X-ray diffractometer (Rigaku RINT-1400) with Cu Kα radiation (λ = 0.154 nm) at room temperature. Infrared spectra were obtained with an IR spectrometer (Perkin Elmer model 1600) at room temperature using a pressed disk composed of a mixture of the samples and KBr. The magnetic susceptibility was collected on a SQUID magnetometer (Quantum Design MPMS-5) with a magnetic field (H) of 1 kG. After the sample was evacuated at 323 K for 1 h, the temperature of the sample was swept from 300 K to 2 K.

Elemental analysis of the compound was performed by Mikroanalytisches Labor Pascher (Germany) for V, P, C, and H. The oxygen content in the sample was calculated by subtracting the sum of the weights of V, P, C, and H. Prior to the analysis, the sample was evacuated at 323 K for 24 h. The average oxidation number of V was determined by a redox titration method using $KMnO_4$ and $FeSO_4(NH_4)_2SO_4 \cdot 6H_2O$ according to the literature.[26] The surface area was measured by a BET method with an automatic adsorption system (BELSORP 28SA, BEL Japan Inc.). SEM images were taken with a scanning electron microscope (HITACHI S-2100).

A thermogravimetric analysis (TG/DTA) was performed using a TG/DTA 200 of Seiko Instruments. After the sample was pretreated in a flow of dried air (50 cm^3 min^{-1}) at 323 K for 24 h, the temperature of the sample was raised to 853 K at a rate of 5 K min^{-1}.

The temperature-programmed decomposition of VAP–*methanol* was carried out using a flow system. Sample powder (10 mg) was placed in a flow reactor (Pyrex-tube, 6 mm of inside diameter) and pretreated in a flow of dried air (10 cm^3 min^{-1}) at 323 K for 24 h. The temperature was raised from 323 K to 493 K at a rate of 5 K min^{-1}, and molecules desorbed from the sample were collected in a U-shaped tube at 77 K. The trapped molecules were then analyzed by a gas chromatograph (TCD (GL science, GC-380)) equipped with a Chromosorb 105 column.

Catalytic Oxidation of Butane. The catalytic oxidation of butane was carried out in a fixed-bed reactor (Stainless tube, 10 mm of inside diameter) under atmospheric pressure at 703 K. Prior to the reaction, vanadyl alkylphosphates were calcined in a flow of a mixture of O_2 (10%) and N_2 (90%) for 2 h. The calcination temperature was adjusted to 703 K for VAP–*methanol*, VAP–*2-propanol*, and VAP–*2-butanol*, and 803 K for VAP–*1-butanol*, VAP–*1-octanol*, and VAP–*cyclopentanol*. These calcination temperatures approximately correspond to the end temperatures of the weight decrease on the TG profiles. The obtained catalysts are denoted by VPO(*alcohol name*). $VOHPO_4 \cdot 0.5H_2O$ was treated in a flow of N_2 at 823 K for 2 h.

A reaction mixture consisting of 5.0% butane, 20% O_2, and N_2 (balance) was fed to the catalyst (1.5 g) at a rate of 30 cm^3 min^{-1}, and the temperature of the reactor was raised from room temperature to 703 K at a rate of 5 K min^{-1}. Since the stationary activity and selectivity were obtained after about 25 h of the reaction at 703 K, the data were collected at 30 h of the reaction. The products were analyzed with on-line gas chromatographs (FID (Shimadzu 14A or Shimadzu 9A) and TCD (Shimadzu 9A)). For butane and MA, a Porapak QS column (inside diameter 2.2 mm, length 1 m) was used. A Molecular Sieve 13X column (inside diameter 2.2 mm, length 4 m) was utilized for O_2, N_2 and CO and a Porapak N column (inside diameter 2.2 mm, length 2 m) for CO_2. CO and CO_2 were converted to methane using a Methanizer (Shimadzu MTN-1) for an FID analysis.

Results

Vanadyl Alkylphosphates Obtained from Primary Aliphatic Alcohols. Table 1 summarizes the results of an elemental chemical analysis for the vanadyl alkylphosphates from primary aliphatic alcohols (abbreviated as VAPs–*Pri*). The P/V ratios of all compounds were 1.00 ± 0.03. Expectedly, the C/P ratio increased as the carbon number of the starting alcohol increased. The R/P ratios calculated from the C/P ratios were 1.00 ± 0.11, where R shows an alkyl group. The oxidation numbers of V in these compounds were determined to be 4.00 ± 0.02.

The IR spectra of VAPs–*Pri* are shown in Fig. 1. The IR bands at around 900–1300 cm^{-1} are due to the lattice vibration of the V–P–O layers of these compounds. The bands of 1192, 1095, and 1054 cm^{-1} are assigned to $\nu(PO_3)$, and that at 981 cm^{-1} is due to $\nu(V{=}O)$.[29] The vibrations of the P–O–C bond were detected at around 1161 cm^{-1} as shoulder peaks.[30] The C–H vibration of the alkyl groups appeared at 2850–3000 cm^{-1}, where the intensities of these bands greatly depended on the kinds of alkyl groups. Furthermore, two bands at 3528 and 3581 cm^{-1} are assignable to free OH stretching.[31]

TG/DTA profiles of VAPs–*Pri* are illustrated in Fig. 2. As shown in Fig. 2a, the weight decreased in two steps for VAP–*methanol*. The first weight loss was observed below 490 K with a slight endothermic, and the second one, above 570 K, was exothermic. The molecules desorbed from VAP–*methanol*, measured by the temperature-programmed decomposition, were mostly methanol (97 mol%) and a small amount of water. As

Table 1. Elemental Chemical Analysis for Vanadyl Alkylphosphates Synthesized from Primary Aliphatic Alcohols

Alcohol	Elemental analysis/wt%[a]					Atomic ratio	Atomic ratio	Formula
	V	P	C	H	O[b]	of P/V	of C/P	
Methanol	28.1	17.4	6.5	2.0	46.1	1.02	0.96	$VO\{(CH_3)_{0.5}/H_{0.5}\}PO_4 \cdot (CH_3OH)_{0.5}$
	(27.4)	(16.7)	(6.5)	(2.2)	(47.3)			
Ethanol	24.8	15.1	12.8	3.1	44.2	1.00	2.19	$VO\{(C_2H_5)_{0.7}/H_{0.3}\}PO_4 \cdot (C_2H_5OH)_{0.4}$
	(25.4)	(15.4)	(13.2)	(3.1)	(43.0)			
1-Propanol	25.0	15.0	15.6	3.3	41.1	0.99	2.68	$VO\{(n\text{-}C_3H_7)_{0.6}/H_{0.4}\}PO_4 \cdot (n\text{-}C_3H_7OH)_{0.3}$
	(24.8)	(15.1)	(15.8)	(3.2)	(41.2)			
1-Butanol	23.3	14.3	21.1	4.2	37.2	1.01	3.81	$VO\{(n\text{-}C_4H_9)_{0.7}/H_{0.3}\}PO_4 \cdot (n\text{-}C_4H_9OH)_{0.3}$
	(22.7)	(13.8)	(21.4)	(4.3)	(37.8)			
1-Hexanol	19.3	12.0	30.5	6.0	32.2	1.02	6.56	$VO\{(n\text{-}C_6H_{13})_{0.6}/H_{0.4}\}PO_4 \cdot (n\text{-}C_6H_{13}OH)_{0.5}$
	(19.3)	(11.7)	(30.0)	(5.7)	(33.3)			
1-Octanol	17.3	10.2	34.4	6.8	31.3	0.97	8.71	$VO\{(n\text{-}C_8H_{17})_{0.6}/H_{0.4}\}PO_4 \cdot (n\text{-}C_8H_{17}OH)_{0.5}$
	(17.3)	(10.5)	(35.8)	(6.6)	(29.8)			

a) The figures in parentheses are the values calculated from the formulae. b) The oxygen content was estimated by subtracting the sum of weights of V, P, C, and H.

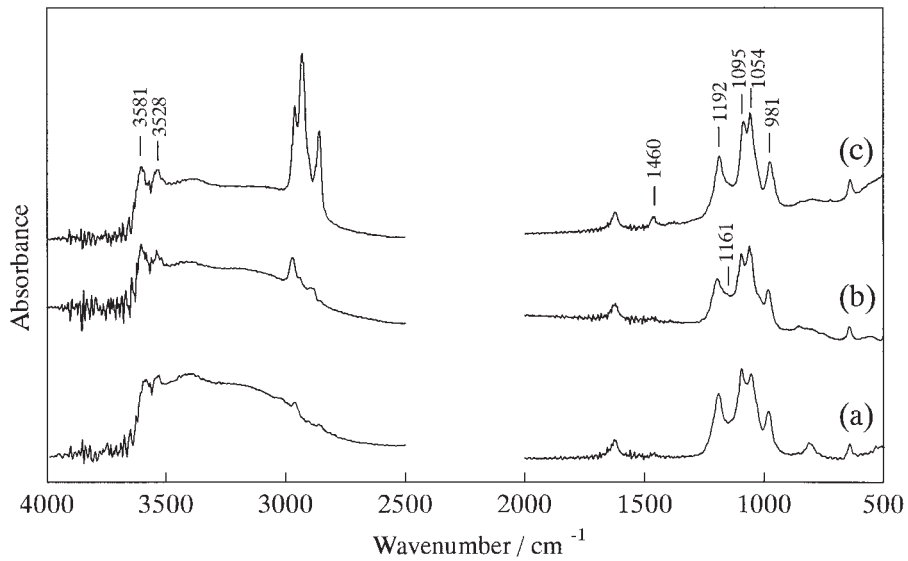

Fig. 1. Infrared spectra of vanadyl alkylphosphate obtained from (a) methanol, (b) 1-propanol, and (c) 1-octanol.

discussed below, the first and second weight losses correspond to the desorption of intercalated methanol and the combustion of the methyl group connected by a covalent bond, respectively. The TG profiles of other VAPs–*Pri* showed loose changes (Fig. 2b–d). Sharp exothermic peaks were detected above 500 K for all of the compounds, and the magnitudes of the peaks increased with an increase in the carbon number of the alcohol.

Figure 3 presents the XRD patterns of VAPs–*Pri*. All of the compounds gave intense diffraction lines at less than 10° of 2θ. The compounds from smaller alcohols, such as methanol, ethanol, and 1-propanol, showed similar XRD patterns (Figs. 3a–c). On the other hand, VAP–*1-butanol*, VAP–*1-hexanol* and VAP–*1-octanol* gave typical patterns due to lamellar compounds (Figs. 3d–f). For example, VAP–*1-octanol* (Fig. 3f) has reflections at $2\theta = 3.72°$ (2.37 nm), 7.38° (1.20 nm), 11.00° (0.80 nm), and 14.68° (0.60 nm), which were assignable to the (001), (002), (003), and (004) reflections of the lamellar phase, respectively. The basal spacings (d(001)) were estimated from 2θ of the (001) reflections to be 0.91 nm (VAP–*methanol*), 1.04 nm (VAP–*ethanol*), 1.23 nm (VAP–*1-propanol*), 1.54 nm (VAP–*1-butanol*), 1.93 nm (VAP–*1-hexanol*), and 2.37 nm (VAP–*1-octanol*), respectively. The d(001) value increased as the carbon number of the starting alcohol increased.

Figure 4 provides a correlation between the d(001) value and the molecular length of the starting alcohol. The molecular length represents the distance between the H atom of OH ($H_{\text{-OH}}$) and the remotest H atom from $H_{\text{-OH}}$, and was estimated based on the covalent bond lengths with MOPAC (FUJITSU, WinMOPAC Version 1.0). It was found that the d(001) values increased in proportion to the length of the alcohol.[25]

Figure 5 shows the dependencies of the magnetic susceptibility on the temperature of the samples for VAP–*methanol* (Fig. 5a) and VAP–*1-octanol* (Fig. 5b). The existence of exchange-coupled V^{4+} dimers in various V–P oxides was confirmed from the magnetic susceptibility.[5,11,32] When the temperature decreased from 300 K, χ_g gradually increased, and then decreased through a maximum at around 45 K. These changes were similar to those of $VOHPO_4 \cdot 0.5H_2O$[5] and $VOHPO_3 \cdot 1.5H_2O$[32] in the

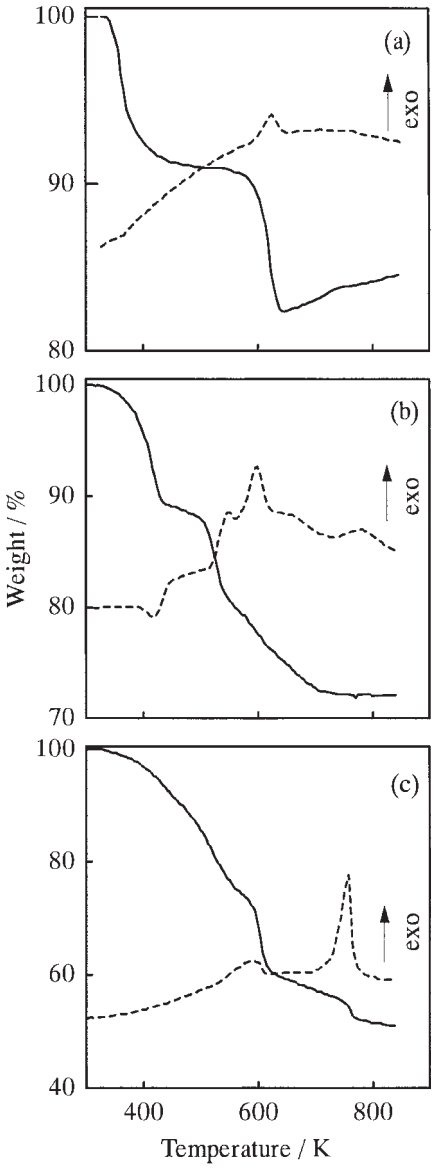

Fig. 2. TG/DTA profiles of vanadyl alkylphosphates measured in air. The vanadyl alkylphosphates were obtained from (a) methanol, (b) 1-propanol, and (c) 1-octanol.

literature, which have V^{4+} dimers. These results indicate the presence of the V^{4+} dimers in the vanadyl alkylphosphates. The data can be analyzed by the Bleaney–Bowers expression (Eq. 1) for an isolated dimer model in which each cation has 1/2 spin, and the g tensors of the cations are isotopic:[33]

$$\chi = \chi_0 + C_i/(T-\theta) + 4C_d/(T(3+\exp(-2J/k_BT))), \quad (1)$$

where χ_0 is a temperature-independent parameter; C_i and θ are the constants associated with the magnetic impurities (i.e. the residual isolated paramagnetic V^{4+} monomers); T is the temperature; C_d is a Curie constant associated with the V^{4+} dimer; J is a coupling constant within the V^{4+} dimer; and k_B is Boltzman's constant. The results of a least-squares fit over the whole temperature range are shown in Fig. 5 (solid line), and the parameters are listed in Table 2 along with the data for $VOHPO_4 \cdot 0.5H_2O$.

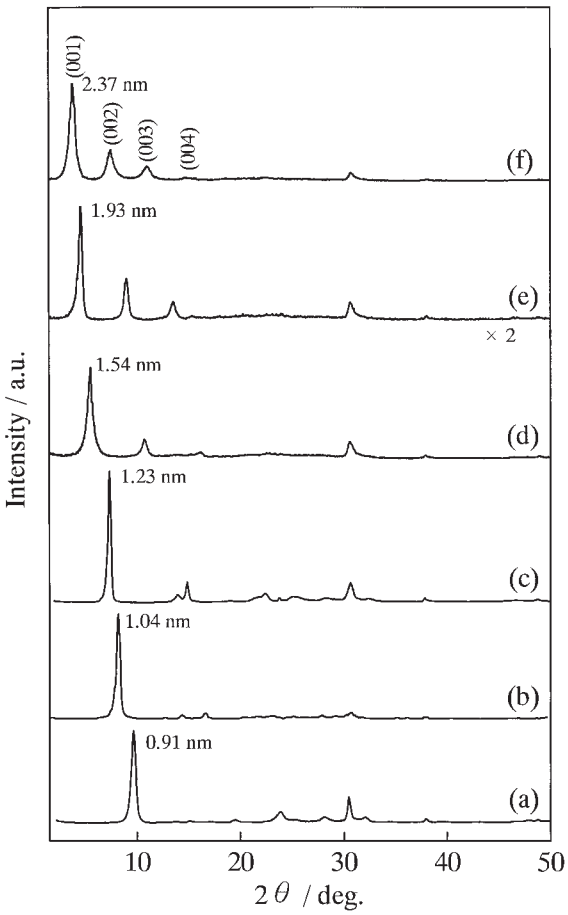

Fig. 3. XRD patterns of vanadyl alkylphosphates obtained from (a) methanol, (b) ethanol, (c) 1-propanol, (d) 1-butanol, (e) 1-hexanol, and (f) 1-octanol.

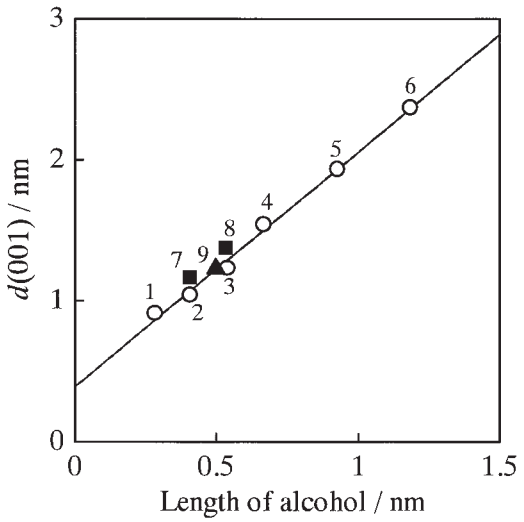

Fig. 4. Correlation between the d(001) values of vanadyl alkylphosphates and length of the starting alcohol. The vanadyl alkylphosphates were obtained from primary aliphatic alcohol (○) (1) methanol, (2) ethanol, (3) 1-propanol, (4) 1-butanol, (5) 1-hexanol, (6) 1-octanol; secondary aliphatic alcohol (■) (7) 2-propanol, (8) 2-butanol; and alicyclic alcohol (▲) (9) cyclopentanol.

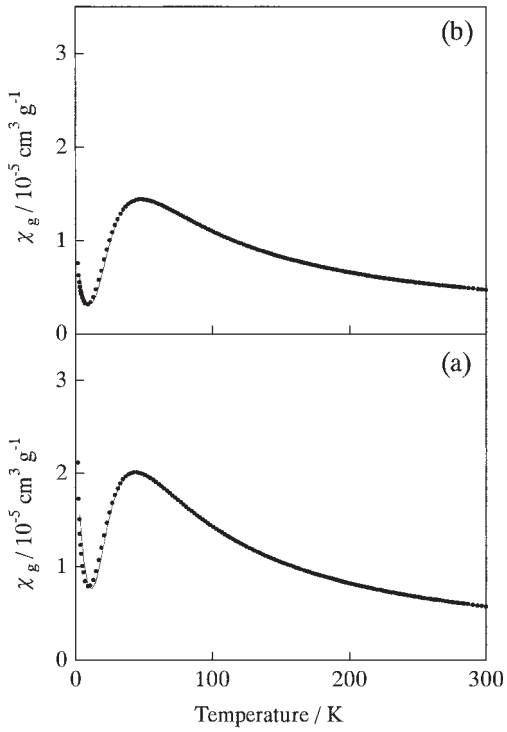

Fig. 5. Magnetic susceptibility of vanadyl alkylphosphates obtained from (a) methanol and (b) 1-octanol. Solid lines represent the result simulated by using the Bleaney–Bowers expression.

Vanadyl Alkylphosphates Obtained from Secondary Aliphatic and Alicyclic Alcohols. The compositions of VAP–*2-propanol*, VAP–*2-butanol*, and VAP–*cyclopentanol* are listed in Table 3. The P/V ratios were close to unity in all of the compounds. The R/P ratios of VAP–*2-butanol* and VAP–*2-propanol* were 0.98 and 0.88, respectively. On the other hand, the ratio of VAP–*cyclopentanol* was 0.55. The oxidation number of V for these vanadyl alkylphosphates was 4.00 ± 0.04.

Figure 6 shows the XRD patterns of VAP–*2-propanol*, VAP–*2-butanol*, and VAP–*cyclopentanol*. These compounds gave intense lines at less than $2\theta = 10^\circ$. For VAP–*2-propanol* (Fig. 6a), a weak diffraction line ($2\theta = 6.7^\circ$) at a slightly lower 2θ angle of the intense one ($2\theta = 7.6^\circ$) was observed. Since the diffraction line assigned to the (200) was observed at 13.8°, this phase is probably a contaminant lamellar phase. The d(001) values were 1.16 nm (VAP–*2-propanol*), 1.37 nm (VAP–*2-butanol*), and 1.23 nm (VAP–*cyclopentanol*), respectively. The correlation between the d(001) value and the molecular length of the starting alcohol was in good accordance with that for VAPs–*Pri* (Fig. 4).

The magnetic susceptibility of VAP–*2-propanol* and VAP–*cyclopentanol* (not shown) gave a maximum of χ_g of around 45 K, as well showing the presence of the V^{4+} dimers in these compounds. The data could be well fitted to the Bleaney–Bowers expression (Eq. 1). The obtained parameters are listed in Table 2. As shown in Fig. 7, VAP–*2-butanol* showed a distinctly different profile of magnetic susceptibility. When the temperature decreased from 300 K, χ_g monotonously increased. The data were well fitted to the Curie–Weiss expression,

$$\chi_g = \chi_0 + C/(T - \theta), \quad (2)$$

for the whole temperature range, as listed in Table 2 and Fig. 7 (solid line). As discussed below, VAP–*2-butanol* has isolated V^{4+} monomers.

As shown in Fig. 8, the IR spectra of VAP–*2-propanol* (Fig.

Table 2. Parameters Used to Fit the Magnetic Susceptibility of Vanadyl Alkylphosphates Synthesized from Various Alcohols and $VOHPO_4 \cdot 0.5H_2O$

Alcohol	χ_0	C_i	θ	C_d	C	J	μ_{eff}
	10^{-7} cm^3 K g^{-1}	10^{-5} cm^3 K g^{-1}	deg	10^{-3} cm^3 K g^{-1}	10^{-3} cm^3 K g^{-1}	cm^{-1}	μ_B
$VOHPO_4 \cdot 0.5H_2O$[a]	2.5	15.3	−0.6	1.99	—	−30.6	1.72
Methanol	0.8	9.9	−3.4	1.69	—	−26.1	1.63
1-Octanol	5.6	3.0	−2.4	1.31	—	−27.5	1.77
2-Propanol	3.2	5.6	−1.3	1.59	—	−29.5	1.66
Cyclopentanol	0.5	8.1	−0.9	1.70	—	−28.8	1.69
2-Butanol	−15.4	—	−9.1	—	1.86	—	1.90

a) $VOHPO_4 \cdot 0.5H_2O$ which was prepared by the so-called organic solvent method.[27]

Table 3. Elemental Analysis for Vanadyl Alkylphosphates Synthesized from Secondary Aliphatic and Alicyclic Alcohols

Alcohol	Elemental analysis/wt%[a]					Atomic ratio	Atomic ratio	Formula
	V	P	C	H	O[b]	of P/V	of C/P	
2-Propanol	24.3	15.9	16.2	3.5	40.1	1.07	2.64	$VO\{(sec\text{-}C_3H_7)_{0.2}/H_{0.8}\}PO_4 \cdot (sec\text{-}C_3H_7OH)_{0.7}$
	(23.9)	(14.5)	(15.2)	(3.7)	(42.7)			
2-Butanol	21.0	13.7	20.7	4.8	39.8	1.07	3.90	$VO\{(sec\text{-}C_4H_9)_{0.1}/H_{0.9}\}PO_4 \cdot (sec\text{-}C_4H_9OH)_{0.9}$
	(22.0)	(13.4)	(22.5)	(4.7)	(37.4)			
Cyclopentanol	25.4	15.7	16.7	2.8	39.4	1.02	2.74	$VO\{(C_5H_9)_{0.2}/H_{0.8}\}PO_4 \cdot (C_5H_9OH)_{0.4}$
	(24.2)	(14.7)	(17.1)	(3.1)	(40.9)			

a) The figures in parentheses are theoretical values calculated from formulae. b) The oxygen content was estimated by subtracting the sum of weight of V, P, C, and H.

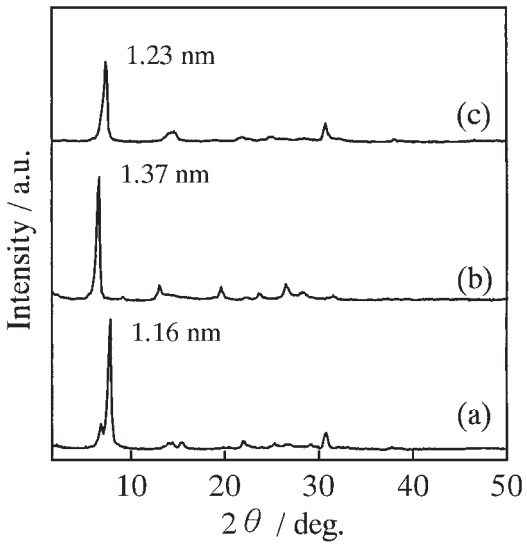

Fig. 6. XRD patterns of vanadyl alkylphosphates obtained from (a) 2-propanol, (b) 2-butanol, and (c) cyclopentanol.

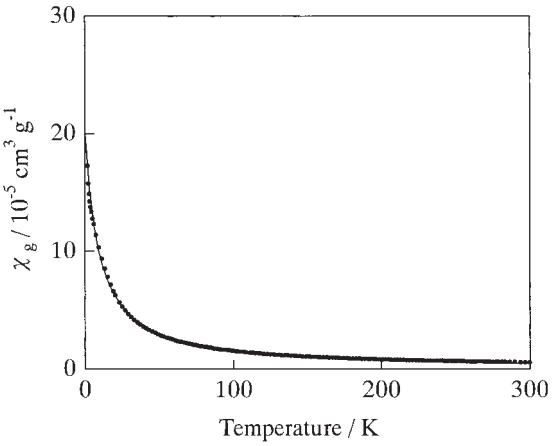

Fig. 7. Magnetic susceptibility of vanadyl alkylphosphate obtained from 2-butanol. Solid line represents the result simulated by using the Curie–Weiss expression.

8a) and VAP–*cyclopentanol* (Fig. 8c) were similar to those of VAPs–*Pri*. On the other hand, VAP–*2-butanol* gave a broad band around 1040 cm^{-1} together with a broad band around 3380 cm^{-1} (Fig. 8b).

TG/DTA profiles of VAP–*2-propanol*, VAP–*2-butanol*, and VAP–*cyclopentanol* are given in Fig. 9. VAP–*2-propanol* and VAP–*cyclopentanol* gave loose changes of weight in the TG profiles (Figs. 9a and c) and indistinct exothermic peaks were observed. On the other hand, the TG profile of VAP–*2-butanol* (Fig. 9b) showed a very sharp weight loss with endothermic peaks at 440 K.

Catalytic Oxidation of Butane. The surface area and the catalytic data are summarized in Table 4. As a reference, the data of a typical $(VO)_2P_2O_7$ catalyst (abbreviated as VPO–*org*)

Table 4. Activity and Selectivity of VP Oxide Catalysts for Oxidation of Butane[a)]

Catalyst[b)]	SA[c)]	Conversion[d)]	Selectivity[d),e)]/%		
	/$m^2\ g^{-1}$	/%	MA	CO_2	CO
VPO(*methanol*)	37.6	59.0	65.3	14.7	20.0
VPO(*1-butanol*)	6.4	21.7	59.3	16.2	23.5
VPO(*1-octanol*)	3.8	15.5	56.7	15.7	27.6
VPO(*2-propanol*)	11.5	34.3	61.6	13.8	24.6
VPO(*2-butanol*)	3.1	16.7	31.0	20.1	48.9
VPO(*cyclopentanol*)	21.2	58.9	68.0	13.4	18.6
VPO(*isobutanol*)	5.2	13.2	43.2	21.6	35.2
VPO–*org*[f)]	43.5	68.9	66.0	15.8	18.3

a) The reaction was performed at 703 K with the mixture of 5.0% butane, 20% O_2, and N_2 (balance). W/F (catalyst weight/flow rate) was 373 g h (mol of butane)$^{-1}$. b) The precursors were previously calcined in a flow of a mixture of 10% O_2 and N_2 (balance) for 2 h at 703 K (VAP–*methanol*, VAP–*2-propanol*, VAP–*2-butanol*), 803 K (VAP–*1-butanol*, VAP–*1-octanol*, VAP–*cyclopentanol*). c) Surface area after the reaction. d) Stationary values obtained after 30 h of the reaction. e) Selectivity based on butane. f) VPO–*org* which was prepared by the so-called organic solvent method.[27]

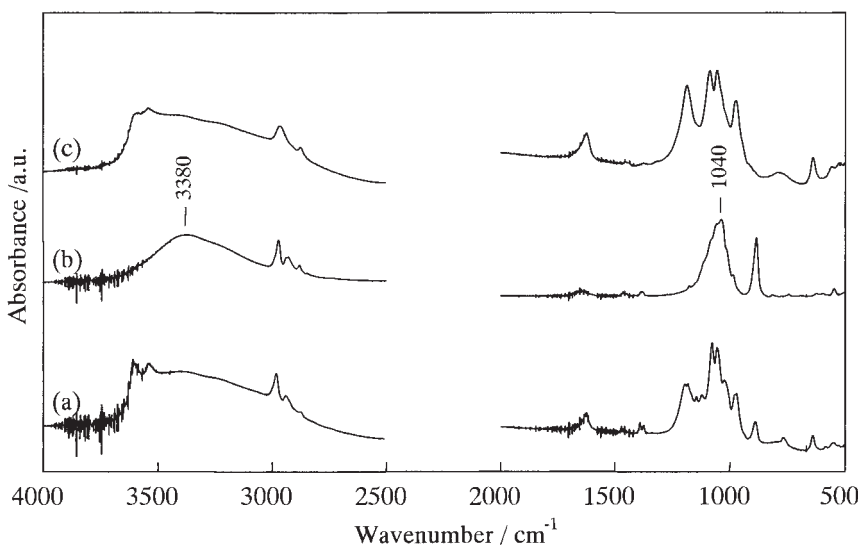

Fig. 8. Infrared spectra of vanadyl alkylphosphate obtained from (a) 2-propanol, (b) 2-butanol, and (c) cyclopentanol.

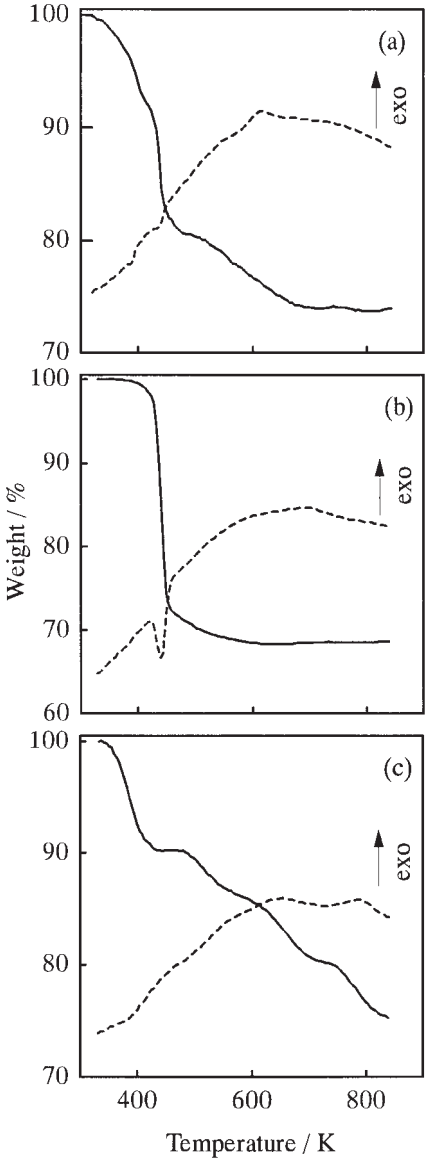

Fig. 9. TG/DTA profiles of vanadyl alkylphosphates measured in air. The vanadyl alkylphosphates were obtained from (a) 2-propanol, (b) 2-butanol, and (c) cyclopentanol.

obtained from $VOHPO_4 \cdot 0.5H_2O$ are shown. The catalytic activity differed significantly depending on the kind of precursors. VPO(*methanol*) and VPO(*cyclopentanol*) were highly active because of the high surface areas, e.g., 37.6 and 21.2 $m^2 g^{-1}$, respectively. VPO(*1-octanol*) and VPO(*2-butanol*), having surface areas less than 4 $m^2 g^{-1}$, showed low activities for the reaction. VPO(*methanol*) and VPO(*cyclopentanol*) exhibited selectivities comparable to that of VPO–*org*. VPO(*1-butanol*), VPO(*1-octanol*), and VPO(*2-propanol*) are slightly less selective than VPO(*methanol*) and VPO(*cyclopentanol*). On the other hand, VPO(*2-butanol*) gave low selectivity (31.0% at 16.7% conversion).

Powder XRD patterns of the catalysts after the reactions are given in Fig. 10. These samples gave basically the patterns of $(VO)_2P_2O_7$, except for VPO(*2-butanol*) (Fig. 10e). VPO(*methanol*), VPO(*cyclopentanol*), and VPO–*org* were assigned to highly crystallized $(VO)_2P_2O_7$. VPO(*1-butanol*) and VPO(*1-octanol*)

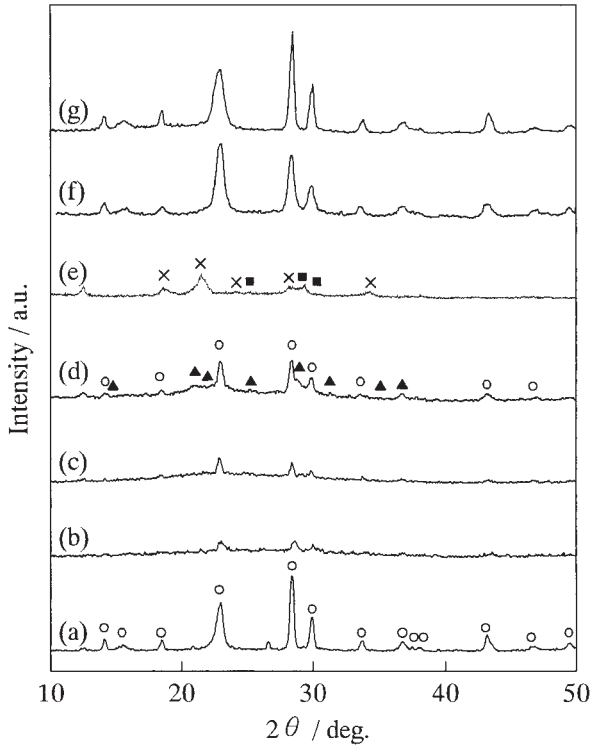

Fig. 10. XRD patterns of vanadium phosphorus oxide catalysts after the oxidation of butane. (a) VPO(*methanol*), (b) VPO(*1-butanol*), (c) VPO(*1-octanol*), (d) VPO(*2-propanol*), (e) VPO(*2-butanol*), (f) VPO(*cyclopentanol*), and (g) VP oxide obtained from $VOHPO_4 \cdot 0.5H_2O$. (○) $(VO)_2P_2O_7$, (▲) γ-$VOPO_4$, (×) X_1 phase, and (■) α-$VOPO_4$.

showed weak diffraction lines of $(VO)_2P_2O_7$ and very broad peaks around $2\theta = 20^\circ$, indicating the presence of an amorphous phase. VPO(*2-propanol*) gave weak diffraction lines of γ-$VOPO_4$, besides medium intense lines of $(VO)_2P_2O_7$. On the other hand, VPO(*2-butanol*) showed only diffraction lines due to α-$VOPO_4$ and the X_1 phase.[34]

SEM images of the catalysts are given in Fig. 11. It was found that the morphology of these compounds changed significantly. VPO(*methanol*) displayed sponge-like shapes consisting of microcrystallites of thin flakes (Fig. 11a). VPO(*1-butanol*) showed bunches of grapes (Fig. 11b). VPO(*cyclopentanol*) displayed a rose-petal morphology, which was shown in q catalyst prepared by the so-called organic solvent method.[27]

Discussion

Structure of Vanadyl Alkylphosphates Synthesized from Primary Aliphatic Alcohols. VAPs–*Pri* have a lamellar structure, because these compounds exhibited a typical XRD pattern of the lamellar phase, as shown in Fig. 3. The linear correlation of the *d*(001) values with the molecular length of the starting alcohol (Fig. 4) indicates that these alkyl groups are present in the interlayer space of these compounds. In other words, VAPs–*Pri* consists of alternating V–P–O layers and organic group ones. In Fig. 4, the value of the intercept, 0.40 nm, of the vertical axis is close to that of $VOPO_4$ (0.411 nm).[35] If the alkyl groups existed as a single or double layer perpendicularly

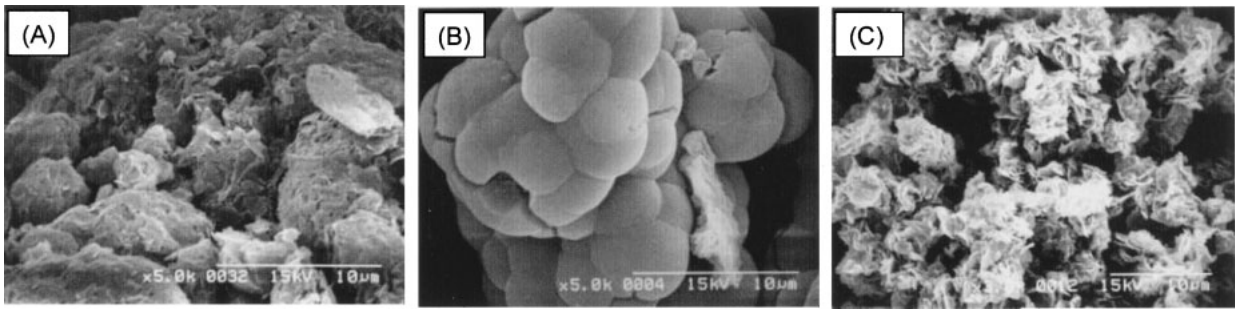

Fig. 11. SEM images of the catalysts after the oxidation of butane. (a) VPO(*methanol*), (b) VPO(*1-butanol*), and (c) VPO(*cyclopentanol*).

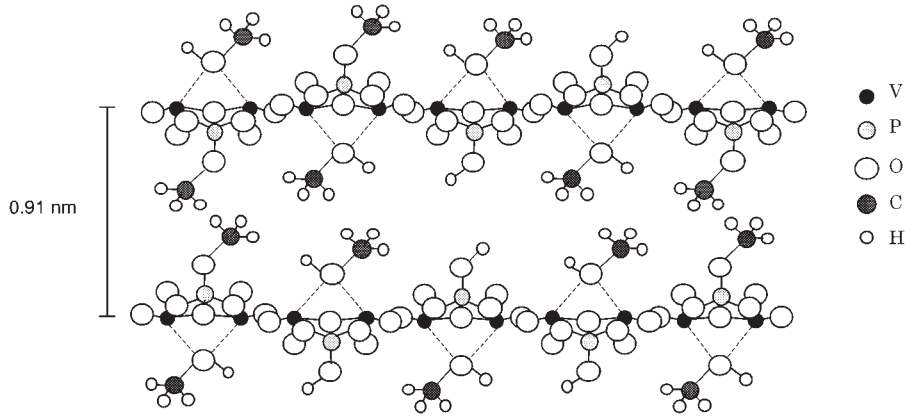

Fig. 12. Proposed model for structure of vanadyl methylphosphate as a typical sample of vanadyl alkylphosphates. The V–P–O layer consists of edge-shared VO_4 dimers connected through corners by $(HO)PO_3$ or $(CH_3O)PO_3$ tetrahedra.

against the V–P–O layer, the slope of the line in Fig. 4 would be 1.0 or 2.0, respectively. Since the observed slope is 1.65, it is deduced that the alkyl groups are present as a double layer with a tilt of about 56° in the interlayer space.

The P/V atomic ratios of VAPs–*Pri* were nearly unity, and the average oxidation numbers of V were very close to +4.0. The absorption bands of $\nu(PO_3)$ and $\nu(V{=}O)$ were observed at almost the same positions as that for $VOHPO_4 \cdot 0.5H_2O$.[5] The magnetic susceptibility (Fig. 5) indicates the existence of V^{4+} dimers in these compounds. In addition, the coupling constants (J) of VAP–*methanol* ($-26.1\ cm^{-1}$) and VAP–*1-octanol* ($-27.5\ cm^{-1}$) were almost the same as that of $VOHPO_4 \cdot 0.5H_2O$ ($-30.6\ cm^{-1}$). The layered $VOHPO_4 \cdot 0.5H_2O$ consists of alternating $VOHPO_4$ layers and H_2O ones. The $VOHPO_4$ layer is made up of edge-shared VO_6 octahedras, V^{4+} dimers, connected through the corners by PO_4 tetrahedras.[5] These results demonstrate that the V–P–O layer of the VAPs–*Pri* is similar to that of $VOHPO_4 \cdot 0.5H_2O$.

The formula of VAP–*methanol* will be discussed first. The IR spectrum showed the vibration of P–O–C ($1161\ cm^{-1}$) for VAP–*methanol* (Fig. 1). Thus, the methyl group would exist as methyl phosphate (P–O–CH_3). Alkyl phosphate is known to be formed by a reaction of P_2O_5 with the corresponding alcohol,[36] supporting the existence of methyl phosphate in this compound. As shown in Fig. 2a, the TG profile showed two-step weight decreases, 8.7 wt% and 8.9 wt%. Since the first decrease was the desorption of methanol and a small amount of water, this weight loss was due to the removal of intercalated methanol. Considering the exothermic behavior at the relatively high temperature, the second weight loss is due to the combustion of methyl group. From these results, the chemical formula of VAP–*methanol* is described as $VO(CH_3O)_x(HO)_{1-x}PO_3 \cdot (CH_3OH)_{1-x}$. Since the C/P ratio of VAP–*methanol* was almost unity (0.96), the chemical formula of VAP–*methanol* was determined to be $VO(CH_3O)_{0.5}(HO)_{0.5}PO_3 \cdot (CH_3OH)_{0.5}$. The composition calculated from this chemical formula is in good agreement with the experimental values, as listed in Table 1. The two weight losses on the TG profile (8.7 wt% and 8.9 wt%) are also consistent with the calculated values (8.4 wt% and 8.7 wt%).

Next, we estimate the chemical formulae of the other VAPs–*Pri*. Similarly to the case of VAP–*methanol*, it was deduced that the exothermic weight losses are due to the combustion of the alkyl group on alkyl phosphate, and that the other weight losses are due to the intercalated alcohol. From this assumption, the chemical formulae of these VAPs–*Pri* were proposed, as listed in Table 1. These formulae are well consistent with the experimental data.

Based on these results, the schematic structure of VAP–*methanol* as a typical sample of VAPs–*Pri* is depicted in Fig. 12. VAPs–*Pri* are lamellar compounds consisting of alternating of V–P–O layers with a thickness of 0.40 nm and alkyl group layers. In this structure, the V–P–O layer is similar to the layer in $VOHPO_4 \cdot 0.5H_2O$, in which the V^{4+} dimers are connected by PO_4 tetrahedra. About half of the total phosphorus is present as alkyl phosphate and the others as hydrogen phosphate (H–O–P–). The alkyl groups of alcohol and alkyl phosphate exist as a double layer with a tilt of about 56°. Since the XRD pattern of VAP–

methanol was not almost unchanged upon a pretreatment at 450 K in air flow, it is presumed that the methyl groups of the methyl phosphate in the adjoining layers are stable and face each other. Two bands due to the free OH vibration observed in the IR spectra (Fig. 1) indicate that the interaction between alcohol and hydrogenphosphate is weak. Probably, the alcohol is located on the V^{4+} dimer and, consequently, apart from the hydrogen phosphates.

Structure of Vanadyl Alkylphosphates Synthesized from Secondary Aliphatic and Alicyclic Alcohols. The P/V ratios and oxidation numbers of V for VAP–*2-propanol*, VAP–*2-butanol* (abbreviated as VAPs–*sec*), and VAP–*cyclopentanol* (abbreviated as VAP–*cycl*) are 1.02–1.07 and 3.99–4.04, respectively, which are very close to those of VAPs–*Pri*. The linear correlation of the *d*(001) value with the length of the alcohol was also observed (Fig. 4), indicating that the branched-alkyl and alicyclic groups in these vanadyl alkylphosphates exist in the same configuration as the straight alkyl groups.

The IR spectra of VAP–*2-propanol* and VAP–*cyclopentanol* were similar to those of VAPs–*Pri*, and the magnetic susceptibility was in accordance with the presence of the V^{4+} dimers (Table 2). It is thus considered that the structure of the V–P–O layer is analogous to those of VAPs–*Pri*. The chemical formulae of these compounds were estimated in a similar manner to VAPs–*Pri* (Table 3). Only 10–20% of phosphorus exists as alkyl phosphate (R–O–P–) in these compounds, while 50–70% of phosphorus was alkyl phosphate in VAPs–*Pri*. Hiyama et al. reported that secondary aliphatic alcohol was readily dehydrated under the presence of P_2O_5.[37] Since P_2O_5 reacts with H_2O to form H_3PO_4, most of the added P_2O_5 was probably converted to H_3PO_4. Consequently, the concentrations of alkyl phosphate formed from the secondary alcohols would be low. It is thus deduced that the incorporation of these alkyl phosphates into VAPs–*sec* and VAP–*cycl* is limited.

Contrary to the above compounds, the structure of the V–P–O layers for VAP–*2-butanol* was different from that of the other vanadyl alkylphosphates. As shown in Fig. 7, the magnetic susceptibility of VAP–*2-butanol* obeyed the Curie–Weiss expression (Eq. 2). Magnetism like this was observed for vanadyl benzylphosphonate[12] and vanadyl *n*-pentylphosphonate[13] with isolated V^{4+} monomers. The IR spectra of VAP–*2-butanol*, having a broad band around 1040 cm^{-1} in the V–P–O lattice vibration region (Fig. 8), was also different from that of other compounds. These broad bands were observed in intercalated $VOPO_4$ compounds having isolated VO_6 octahedra, e.g., $VOPO_4$–aniline,[38] $VOPO_4$–anilinoaniline,[39] and $VOPO_4$–4-butylaniline.[40] These results indicate that the isolated V^{4+} monomers exist in VAP–*2-butanol*. Furthermore, VAP–*2-butanol* gave a broad band of around 3380 cm^{-1} in the IR spectra, suggesting that hydrogenphosphate (POH) of the V–P–O layer interacts with the OH of intercalated 2-butanol.

In summary, the structure of VAP–*2-propanol* and VAP–*cyclopentanol* is the same as those of VAPs–*Pri*, while the $ROPO_3/HOPO_3$ ratios are smaller than those in VAPs–*Pri*. On the other hand, VAP–*2-butanol* has a different structure from that of the above compounds, and has isolated V^{4+} monomers linked with PO_4 tetrahedra.

Selective Oxidation of Butane with the Catalysts Obtained from Vanadyl Alkylphosphates. Highly crystalline $(VO)_2P_2O_7$ phases were obtained from VAP–*methanol* and VAP–*cyclopentanol* by calcination, followed by activation under the reaction conditions for 30 h. These vanadyl alkylphosphates with a structure containing V^{4+} dimers were transformed to $(VO)_2P_2O_7$. On the other hand, only VAP–*2-butanol* having isolated V^{4+} monomers changed to a mixture of α-$VOPO_4$ and X_1 phases instead of $(VO)_2P_2O_7$. Such a difference in the resulting phases would be caused by the difference in the structures of the V–P–O layers of the vanadyl alkylphosphates. VAP–*1-butanol* and VAP–*1-octanol* were transformed to less-crystalline $(VO)_2P_2O_7$ with amorphous V–P oxides. VAP–*1-butanol* and VAP–*1-octanol* gave large exothermic peaks above 500 K in TG/DTA, as compared with that for VAP–*methanol* and VAP–*cyclopentanol* (Fig. 2). Therefore, the amorphous V–P oxides would arise from local temperature excursions resulting from the exothermic combustion of these alkyl phosphates.

The concentrations of butane used for commercial processes are usually about 1.5 vol% and 4.0 vol% for fixed-bed and fluidized-bed reactor, respectively. From an industrial viewpoint, operation under higher concentrations of butane is preferred for a higher space-time yield of MA. Thus, catalytic oxidation was performed at 5.0 vol% of butane.

VPO(*methanol*) and VPO(*cyclopentanol*) showed high catalytic activities and selectivities to MA (Table 4). The catalytic performances of these catalysts were comparable to that of VPO–*org* (66% of selectivity), which was reported to be selective at 5% of butane.[41] On the other hand, the selectivities of VPO(*1-butanol*), VPO(*1-octanol*), and VPO(*2-propanol*) were not high (about 60%) and that of VPO(*2-butanol*) was low (31% at 16.7% conversion).

Shimoda et al. reported that the $VOPO_4$ phases of V^{5+}, such as α-$VOPO_4$ and β-$VOPO_4$, as well as the amorphous and X_1 phases, were less selective than $(VO)_2P_2O_7$.[34] Therefore, the low selectivity of VPO(*2-butanol*) is due to the presence of X_1 and α-$VOPO_4$, predominantly. It is also considered that the presence of amorphous V–P oxides or γ-$VOPO_4$ is responsible for the relatively low selectivities of VPO(*1-butanol*), VPO(*1-octanol*), and VPO(*2-propanol*). On the other hand, the high selectivities of VPO(*methanol*) and VPO(*cyclopentanol*) are due to the single phase of $(VO)_2P_2O_7$.

It is known that the catalytic performance greatly depends on the morphology of the catalyst as well. Catalysts consisting of microcrystallites of thinner plates showed high selectivities to MA,[42] because of a preferential exposure of the (100) plane of $(VO)_2P_2O_7$. The relatively high selectivities of VPO(*methanol*) and VPO(*cyclopentanol*) would be due to their thinner plate-like shapes (Fig. 11a,c).

Conclusion

The present study clarified the structure of the vanadyl alkylphosphates by using various characterization techniques. The vanadyl alkylphosphates have a lamellar structure and the alkyl groups exist as a double layers with a tilt of about 56° against the V–P–O layer. The structure of the V–P–O layers is similar to that of $VOHPO_4 \cdot 0.5H_2O$, having the V^{4+} dimers connected by PO_4 tetrahedra, except for vanadyl *sec*-butylphosphate. In vanadyl *sec*-butylphosphate, isolated VO_6 monomers exist. The $(ROPO_3)$/(total P) ratios were 0.5–0.7 for the vanadyl alkylphosphates obtained from primary aliphatic alcohols and 0.1–0.2

for that from secondary aliphatic and alicyclic alcohols. Well-crystallized $(VO)_2P_2O_7$ catalysts were obtained from vanadyl methylphosphate and vanadyl cyclopentylphosphate. These catalysts showed both high catalytic activity and selectivity to MA under a high concentration of butane, which was comparable to that of catalysts prepared by the so-called organic solvent method.

This work was supported by the New Energy and Industrial Technology Development Organization (NEDO) and Japan Chemical Industry Association (JCIA). We thank Dr. H. Sato (Tokyo Institute of Technology) for the measurement and analysis of the magnetic susceptibility.

References

1 S. Albonetti, F. Cavani, and F. Trifirò, *Catal. Rev. —Sci, Eng.*, **38**, 413 (1996).
2 G. J. Hutchings, *Appl. Catal.*, **72**, 1 (1991).
3 B. K. Hodnett, *Catal. Rev. Eng.*, **17**, 373 (1985).
4 G. Centi, F. Trifirò, J. R. Ebner, and V. M. Franchetti, *Chem. Rev.*, **88**, 55 (1988).
5 J. W. Johnson, D. C. Johnston, A. J. Jacobson, and J. F. Brody, *J. Am. Chem. Soc.*, **106**, 8123 (1984).
6 E. Bordes and P. Courtine, *J. Solid State Chem.*, **55**, 270 (1984).
7 S. Tomita, T. Ihara, and H. Suwa, *Jpn. Kokai Tokkyo Koho*, 5-261292 (1993) to Mitsuikasei Kogyo.
8 I. Sawa, H. Suwa, and Y. Ishii, *Jpn. Kokai Tokkyo Koho*, 11-92973 (1999) to Mitsubishi Kagaku.
9 T. A. Byser Jr., *Jpn. Kokai Tokkyo Koho*, 58-69577 (1983) to EI Du Pont de Memous and Company.
10 S. H. Horowitz, WO Patent 98/15353 (1998) to EI Du Pont de Memous and Company.
11 V. V. Guliants, J. B. Benziger, S. Sundaresan, I. E. Wachs, and J.-M. Jehng, *Chem. Mater.*, **7**, 1493 (1995).
12 J. W. Johnson, A. J. Jacobson, J. F. Brody, and J. T. Lewandowski, *Inorg. Chem.*, **23**, 3842 (1984).
13 G. Huan, J. W. Johnson, J. F. Brody, D. P. Goshorn, and A. J. Jacobson, *Mater. Chem. Phys.*, **35**, 199 (1993).
14 G. Huan, A. J. Jacobson, J. W. Johnson, and D. P. Goshorn, *Chem. Mater.*, **4**, 661 (1992).
15 E. M. Sabbar, M. E. de Roy, A. Ennaqadi, C. Gueho, and J. P. Besse, *Chem. Mater.*, **10**, 3856 (1998).
16 J. W. Johnson, J. F. Brody, and R. M. Alexander, *Chem. Mater.*, **2**, 198 (1990).
17 N. Mizuno, H. Hatayama, S. Uchida, and A. Taguchi, *Chem. Mater.*, **13**, 179 (2001).
18 T. Doi and T. Miyake, *Chem. Commun. (Cambridge)*, **1996**, 1635.
19 T. Abe, A. Taguchi, and M. Iwamoto, *Chem. Mater.*, **7**, 1429 (1995).
20 M. Roca, J. E. Haskouri, S. Cabrera, A. B. Porter, J. Alamo, D. B. Porter, M. D. Marcos, and P. Amorós, *Chem. Commun. (Cambridge)*, **1998**, 1883.
21 H. Hatayama, M. Misono, A. Taguchi, and N. Mizuno, *Chem. Lett.*, **2000**, 884.
22 N. Hiyoshi, N. Yamamoto, N. Terao, T. Nakato, and T. Okuhara, *Stud. Surf. Sci. Catal.*, **130**, 1715 (2000).
23 N. Hiyoshi, N. Yamamoto, and T. Okuhara, *Chem. Lett.*, **2001**, 484.
24 T. Nakato, Y. Furumi, and T. Okuhara, *Chem. Lett.*, **1998**, 611.
25 Y. Kamiya, E. Nishikawa, A. Satsuma, N. Mizuno, and T. Okuhara, *Sekiyu Gakkaishi*, **44**, 265 (2001).
26 B. K. Hodnett, P. Permanne, and B. Delmon, *Appl. Catal.*, **6**, 231 (1983).
27 H. Igarashi, K. Tsuji, T. Okuhara, and M. Misono, *J. Phys. Chem.*, **97**, 7065 (1993).
28 F. Cavani, G. Centi, and F. Trifirò, *Ind. Eng. Chem. Prod. Res. Des.*, **22**, 570 (1983).
29 G. Basca, F. Cavani, G. Centi, and F. Trifirò, *J. Catal.*, **99**, 400 (1986).
30 L. J. Bellamy, ''The Infra-red Spectra of Complex Molecules,'' Chapman and Hall, London (1975), Vol. 1, p. 354.
31 L. J. Bellamy, ''The Infra-red Spectra of Complex Molecules,'' Chapman and Hall, London (1975), Vol. 1, p. 109.
32 V. V. Guliants, J. B. Benziger, and S. Sundaresan, *Chem. Mater.*, **7**, 1485 (1995).
33 B. Bleaney and K. D. Bowers, *Proc. R. Soc. London, Ser. A*, **214**, 451 (1952).
34 T. Shimoda, T. Okuhara, and M. Misono, *Bull. Chem. Soc. Jpn.*, **58**, 2163 (1985).
35 E. Bordes, P. Courtine, and G. Pannetier, *Ann. Chim. (Paris)*, **8**, 105 (1973).
36 D. F. Toy, ''Comprehensive Inorganic Chemistry,'' Pergamon Press, Oxford (1968), p. 442.
37 K. Hiyama, M. Suzuki, M. Nakamura, Y. Hatanaka, O. Kobayashi, and M. Higashihara, *Sci. Ind.*, **72**, 89 (1998).
38 H. Nakajima and G. Matsubayashi, *Chem. Lett.*, **1993**, 423.
39 H. Nakajima and G. Matsubayashi, *J. Mater. Chem.*, **5**, 105 (1995).
40 T. Nakato, Y. Furumi, N. Terao, and T. Okuhara, *J. Mater. Chem.*, **10**, 737 (2000).
41 Y. Kamiya, E. Nishikawa, T. Okuhara, and T. Hattori, *Appl. Catal. A*, **206**, 103 (2001).
42 H. S. Horowitz, C. M. Bladostone, A. W. Sleight, and G. Teufer, *Appl. Catal.*, **38**, 193 (1988).